Beam displacement and blur caused by fast electron beam deflection

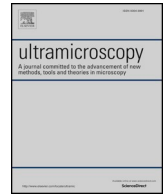Zhang, Lixin; Garming, Mathijs W.H.; Hoogenboom, Jacob P.; Kruit, Pieter

Important note
To cite this publication, please use the final published version (if applicable).
Please check the document version above.

Beam displacement and blur caused by fast electron beam deflection

Lixin Zhang[a,b,*], Mathijs W.H. Garming[b], Jacob P. Hoogenboom[b], Pieter Kruit[b]

[a] *School of Instrumentation and Optoelectronic Engineering, Beihang University, Beijing, 100191, China*
[b] *Department of Imaging Physics, Delft University of Technology, Lorentzweg 1, 2628CJ, Delft, the Netherlands*

ARTICLE INFO

ABSTRACT

Electrostatic beam blankers are an alternative to photo-emission sources for generating pulsed electron beams for Time-resolved Cathodoluminescence and Ultrafast Electron Microscopy. While the properties of beam blankers have been extensively investigated in the past for applications in lithography, characteristics such as the influence of blanking on imaging resolution have not been fully addressed. We derive general analytical expressions for the spot displacement and loss in resolution induced by deflecting the electron beam in a blanker. In particular, we analyze the sensitivity of both measures to how precise the conjugate focus is aligned in between the deflector plates. We then work out the specific case of a beam blanker driven by a linear voltage ramp as was used in recent studies by others and us. The result shows that the spot displacement and focus blur can be reduced to the same order as the electron beam probe size, even when using a beam blanker of millimeter or larger scale dimensions. An interesting result is that, by the right choice of the focus position in the deflector, either the spot displacement from the stationary position can be minimized, or the blur can be made zero but not both at the same time. Our results can be used both to characterize existing beam blanker setups and to design novel blankers. This can further develop the field of time-resolved electron microscopy by making it easier to generate pulses with a typical duration of tens of picoseconds in a regular scanning electron microscope at high spatial resolution.

1. Introduction

Electrostatic deflectors are commonly used in electron beam lithography and microscopy to avoid exposure of specific areas of a sample by deflecting, or blanking, the beam over an aperture [1-4]. Fast beam blankers (FBBs), operating with nanoseconds voltage ramps, are a standard asset for electron beam systems. Besides blanking, FBBs have also been used to generate pulsed electron beams, for instance for stroboscopic Scanning Electron Microscopy (SEM) [5,6], or for analyzing signal transmission speeds in integrated circuits [7,8]. Different FBB designs and electron-optical implementations have been realized and experimentally or theoretically investigated, and were found to generate short pulses down to the few picoseconds time scale [9,10]. Recently, FBBs have regained interest as a means to generate electron pulses for ultrafast electron microscopy (UEM) and/or time-resolved cathodoluminescence microscopy (TR-CL) [1,2]. As an FBB is a commercially obtainable insert to existing microscopes, the use of an FBB provides an attractive alternative to allow laser-triggered emission of electron pulses, which requires modification of the electron gun unit. Also, novel concepts based on microfabricated electrostatic deflectors [11,12] or deflecting by resonant magnetic field modes in a microwave

cavity [13-15] have been proposed as a means to generate sub-picosecond pulses using the blanker concept, rivaling the pulse durations achieved with photoemission sources [16].

For applications in stroboscopic UEM or TR-CL, the aim is generally to image at the highest possible resolution. When using conjugate blanking, the beam is kept in focus on the sample during deflection, so that high-resolution imaging can be done [1]. However, there are several factors that may compromise the resolution in blanked mode compared to the continuous beam operation of the SEM. First, in order to have a conjugate focus in between the FBB deflector plates, the electron optical path may have to be adjusted from its optimal configuration, thereby slightly increasing aberrations. Second, increasing the temporal resolution may require using a smaller (tens of μm) blanking aperture at the lower pole piece to reduce the deflection angle for which the beam passes the aperture and thus a pulse is generated; this smaller aperture may also decrease the resolution [2]. Both these effects depend on the design of the SEM in use and could, in principle, be reduced with an optimized column design. Third, the deflection of the beam leads to a displacement of the focal spot in between the blanker plates, which translates to a spot displacement (SD) on the sample (see Fig 1). As this displacement is dependent on the time-

---

* Corresponding author.
  E-mail address: zhanglixin@buaa.edu.cn (L. Zhang).
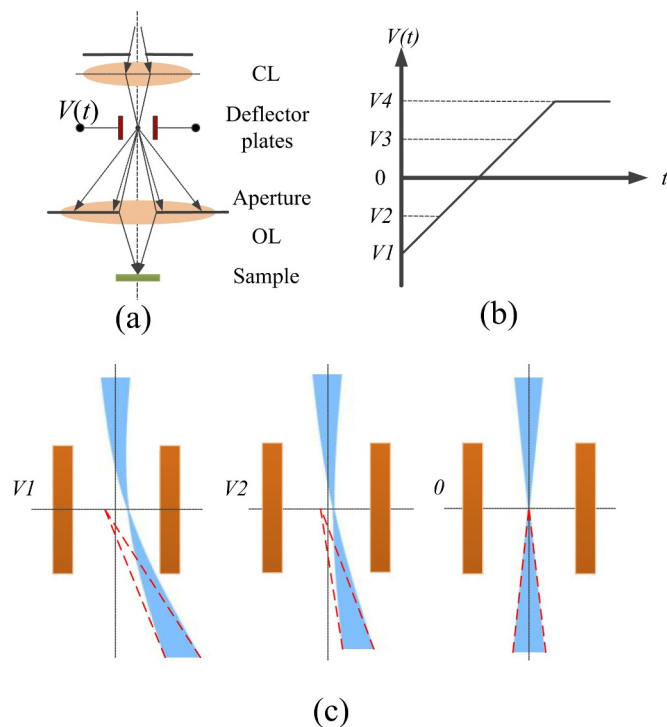
Fig. 1. (a) Schematic configuration of a blanking system with electrostatic deflectors plates. A condenser lens (CL) focuses the beam in between the deflector plates. An aperture is positioned on the axis close to the objective lens (OL). The voltage input V(t) deflects the beam over the aperture generating an electron pulse. (b) Indication of an increasing voltage ramp with the beam deflection by the blanker at stages *V1, V2*, and *0* indicated in (c). In (c) the electron beam is indicated in blue and the apparent retraced focus spot position in the blanker is indicated in red. The magnitude of the resulting spot displacement depends on the arrival time of an electron in the blanker relative to V(t). (For interpretation of the references to color in this figure legend, the reader is referred to the web version of this article.)

varying deflection angle, this leads to a blur in the pulsed electron beam focus. In the literature this has alternatively been denoted as 'spurious deflection' or 'beam motion error', but in the remainder of this manuscript, we will keep using the abbreviation SD.

Paik et al. [17] have made an analytical calculation on the SD of two pairs of blanking plates during beam switching, and analyzed the relation of the SD with the rise time of the signal. Later, trajectory equations were derived in closed form for electrons in time-dependent electric fields by Gesley [10] and he analyzed the resulting beam motion. This framework, however, cannot be readily adopted to a new design or a single pair of deflector plates. Mulder and Kruit [18] derived analytical solutions for the SD resulting from transient signals during conjugate blanking. Recently, Ruan [19] also made a detailed calculation on the SD for single-, double- and quadruple-deflection blankers using a similar geometric method as the one by Gesley [10] and Mulder and Kruit [18]. While the SD has thereby been analyzed in detail, the resulting blur during transient switching has, to our knowledge, not been quantified, especially for the case of a custom FBB consisting of a single pair of mm-sized deflection plates used in SEMs. In addition, it is important to understand how the spot displacement and resulting blur are affected by (mis)alignment of the conjugate focal plane in the center of the blanker plates, which has to be done for each operating voltage and may be hard to establish precisely.

In this paper, we present an analytical evaluation of SD and focus blur induced by a single pair of mm-sized deflector plates. We analyze how both factors depend on the electron energy at the FBB position, the electron entry time with respect to the deflector voltage transient, and the mismatch between the focal plane and the center of the deflector plates. Our results provide insight into the intrinsic resolution limitations imposed by current FBBs and allow to evaluate how SD and resolution loss can be minimized or avoided with current or potentially new designs.

2. Analytical calculation of SD and blur

The basic configuration for a FBB consisting of a single pair of deflector plates is shown in Fig. 1(a). Here, a time-varying voltage, V(t), sweeps the beam over an aperture, thus creating an electron pulse. This configuration was already proposed in 1960 by Fowler and Good [3] and is still the standard configuration for commercial FBBs used recently for time-resolved SEM by us as well as others [1,2]. In operation of this blanking system, typically a square or sinusoidal voltage pulse is used, so that the continuous SEM beam is deflected over an aperture by the rising and/or dropping edge of the pulse, thus generating two electron pulses per cycle. Part of this sequence is schematically indicated in Fig. 1(c), where it can also be seen that the time-dependent deflection leads to a time-dependent displacement of the focus spot in between the blanker plates. This SD translates to a displacement of the focus on the sample, demagnified by the objective lens.

First, we will calculate the magnitude of the SD for conjugate blanking as a function of the arrival time of an electron in the blanker plates following Ruan [19] (see also Fig. 1(c)). Later, this will allow us to derive the induced focus blur on the sample.

Besides the electron arrival time, the total deflection of the electron trajectory is dependent on the flight time t_f in the deflector field, which follows from the length of the deflector plates, L, and the acceleration voltage, Φ from source to blanker:

$$t_f = \frac{L}{v_0} \tag{1}$$

$$v_0 = \sqrt{\frac{2 \cdot q \cdot \Phi}{m_0}} \tag{2}$$

Here q is the elemental charge and m_0 the rest mass of the electron.

In the blanker, the electron experiences a time-dependent lateral acceleration given by:

$$a_x(t) = \begin{cases} \frac{q \cdot V(t)}{m_0 \cdot d} & (t_{en} \leq t \leq t_f + t_{en}) \\ 0 & (t < t_{en} \; or \; t > t_f + t_{en}) \end{cases} \tag{3}$$

where d is the distance between the deflector plates and x denotes the direction perpendicular to the optical axis and the deflector plates (see Fig 2), t_{en} is the entry time of electron and here $t_{en} \geq 0$.

In Fig. 2, we indicate the further definition of parameters relevant to evaluate the SD. Here, Δz denotes the misalignment of the focal plane with respect to the mid-plane of the blanker. At any time $t_{en} < t < t_{en} + t_f$, the electron has acquired a lateral velocity v_x given by:

$$v_x = \int_{t_{en}}^{t} a(t)dt \tag{4}$$

The distance over which the electron has been deflected when exiting the blanker is given by:

$$s = \int_{t_{en}}^{t_f+t_{en}} v(t)dt = \int_{t_{en}}^{t_f+t_{en}} \left(\int_{t_{en}}^{t} a(t)dt \right)dt \tag{5}$$

As the electron now travels with constant lateral velocity v_{ex} (the
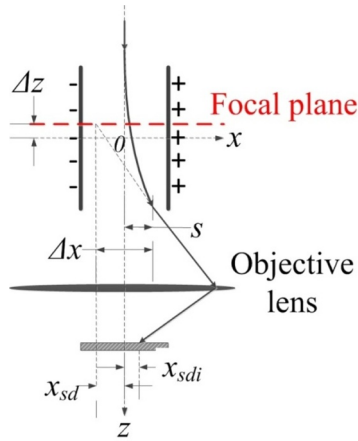
Fig. 2. Schematic configuration of spot displacement with the different confocal spot. x_{sd} is the spot displacement on the focal plane, x_{sdi} is the spot displacement on the sample plane, $x_{sdi} = M \cdot x_{sd}$, with M the demagnification of the objective lens, typically $1/M \sim 20$–30.

lateral velocity with which the electron exits the blanker), we can now find the apparent deflection Δx by tracing the electron back to the focal plane (see also Fig. 2):

$$\Delta x = v_{ex} \cdot \frac{0.5L - \Delta z}{v_0} \tag{6}$$

where the exit velocity, v_{ex}, is given by

$$v_{ex} = \int_{t_{en}}^{t_{en}+t_f} a(t)dt \tag{7}$$

We now get for the spot displacement:

$$x_{sd} = \Delta x - s = \frac{0.5L - \Delta z}{v_0} \cdot \int_{t_{en}}^{t_{en}+t_f} a(t)dt - \int_{t_{en}}^{t_{en}+t_f} \left(\int_{t_{en}}^{t} a(t)dt \right) dt \tag{8}$$

And inserting Eqs. (1) and (2) in Eq. (8), we arrive at:

$$x_{sd} = \frac{(0.5L - \Delta z) \cdot \sqrt{q}}{d \cdot \sqrt{2\phi m_0}} \cdot \int_{t_{en}}^{t_{en}+t_f} V(t)dt - \frac{q}{m_0 d} \int_{t_{en}}^{t_{en}+t_f} \int_{t_{en}}^{t} V(t)dtdt \tag{9}$$

In this equation, we see that besides experimentally well controllable parameters like the dimensions of the beam blanker, the acceleration voltage of the electrons, and the temporal evolution of the voltage pulse, the spot displacement depends on the amount of misalignment of the focal plane with respect to the mid-plane of the blanker and the entry time of the electron in the blanker. If we assume a linear voltage ramp (as indicated in Fig. 1) that rises from V_{min} to V_{max} in time t_r, $V(t) = \frac{\Delta V}{t_r} \cdot t - 0.5\Delta V$, where $\Delta V = V_{max} - V_{min}$, the expression for the spot displacement becomes:

$$x_{sd\_linear} = \frac{\Delta V \cdot L}{2\phi^2 t_r d\sqrt{q}} \left(\frac{L \cdot \sqrt{2\phi m_0}}{4} \left(\frac{L}{6} - \Delta z \right) - \phi\Delta z\sqrt{q}\left(t_{en} - \frac{t_r}{2} \right) \right) \tag{10}$$

As a continuous beam enters the beam blanker, the electron entry times are randomly distributed. In order to evaluate the spot displacement for electrons in the pulsed beam, we only need to consider those electrons that are transmitted by the blanking aperture. This translate to a window of allowed entry times, and depending on the size of this window, the electrons in the pulsed beam will have different SD. This variation in SD within the beam leads to a blur of the focus on the sample.

We denote the duration of the pulse generated by the beam blanker with τ_{pulse}. Then, if the electrons in the front of the pulse arrive at the deflector plates at entrance time t_{en}, electrons at the end of the pulse enter the deflector at $t_{en} + \tau_{pulse}$, as illustrated in Fig. 3. Here, we
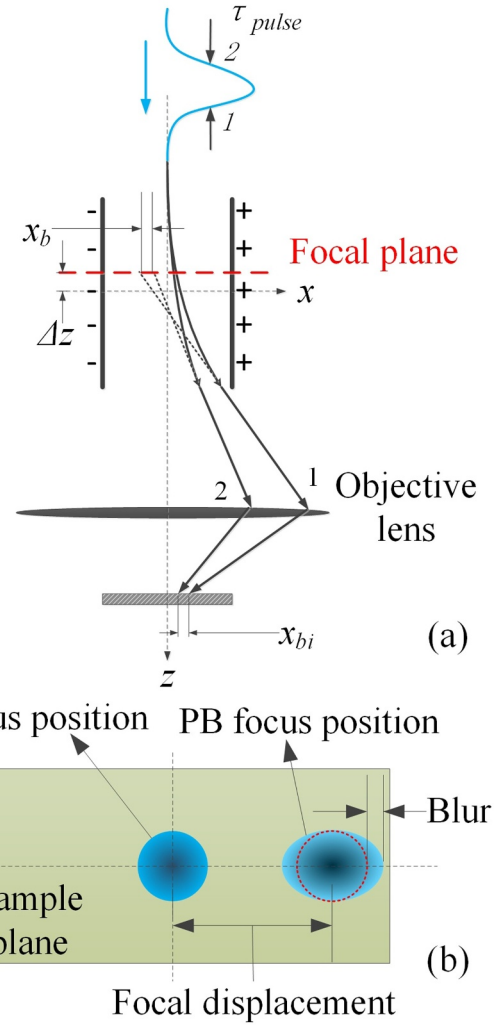

Fig. 3. Schematic indication of blur induced in an electron pulse by a beam blanker. (a) Electrons at the front of the electron pulse, indicated by 1, will undergo a different deflection and thus spot displacement than electrons at the rear of the pulse, indicated by 2. Note that the pulse is defined after the blanking aperture in the objective lens (dark gray) and the sketch indicates a slightly off-axis aperture. The different spot displacements in the pulse lead to a blur in the focus. x_b denotes the blur in the blanker and x_{bi} the blur on the sample plane: $x_{bi} = M \cdot x_b$. (b) Schematic depiction of the influence of blanking on the electron focus on the sample plane. CB: Continuous Beam; PB: Pulsed Beam. The amount of focal spot displacement depends on electrons in the center of the pulse, the blur is determined by the varying spot displacement within the pulse.

assume that the pulse duration is measured by the FWHM of the pulse, calculated as:

$$\tau_{pulse} = \frac{2\phi t_r d (d_{beam} + d_{aperture})}{\Delta V \cdot H \cdot L} \tag{11}$$

where H is the distance between the beam blanker center to the aperture plane, d_{beam} is the diameter of the beam at the aperture plane, $d_{aperture}$ the diameter of the aperture. Note that the precise position of the aperture with respect to the electron optical axis determines the entrance time t_{en} of the first electrons in the pulse. If the blanking aperture is perfectly aligned with respect to the axis, t_{en} and $t_{en} + \tau_{pulse}$ will be equally distributed on both sides of the zero-crossing time of the deflector voltage pulse.

Using Eq. (9), we can now calculate the spot displacement for electrons 1 and 2 at the front and rear of the pulse respectively (see
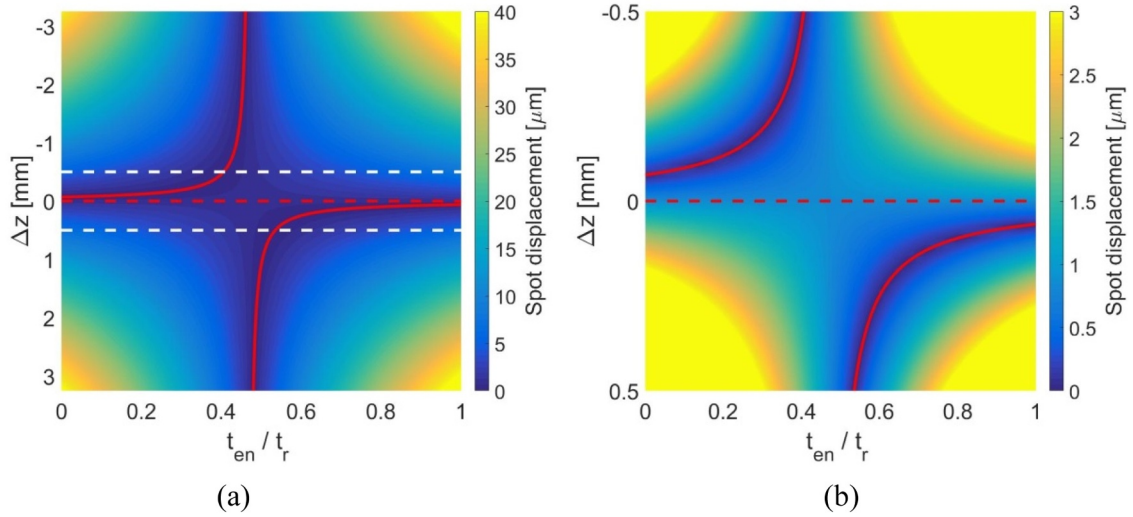
Fig. 4. (a) Spot displacement in between the blanker plates in relation to the relative arrival time in the blanker and the misalignment of the focus with respect to the blanker middle plane. The color map indicates the magnitude of the spot displacement. Calculations with parameters from Ref. [1], with 5 keV electron energy. The red curve in the figure represents the conditions for which the spot displacement equals zero. The dashed red line indicates where the spot displacement remains constant. The two dashed white lines indicate the region shown in (b). In (b), it can be seen that the spot displacement around the middle plane of the beam blanker is about 1 μm. (For interpretation of the references to color in this figure legend, the reader is referred to the web version of this article.)

Fig. 3), where we take entry time t_{en} for electron 1 and $t_{en} + \tau_{pulse}$ for electron 2:

$$x_{sd1} = \frac{0.5L - \Delta z}{v_0} \cdot \int_{t_{en}}^{t_{en}+t_f} a(t)dt - \int_{t_{en}}^{t_{en}+t_f} \left(\int_{t_{en}}^{t} a(t)dt \right) dt \tag{12}$$

$$x_{sd2} = \frac{0.5L - \Delta z}{v_0} \cdot \int_{t_{en}+\tau_{pulse}}^{t_{en}+t_f+\tau_{pulse}} a(t)dt - \int_{t_{en}+\tau_{pulse}}^{t_{en}+t_f+\tau_{pulse}} \left(\int_{t_{en}+\tau_{pulse}}^{t} a(t)dt \right) dt \tag{13}$$

The blur then follows by taking the difference between these two spot displacements:

$$x_b = x_{sd1} - x_{sd2} \tag{14}$$

For the linear voltage ramp, the blur can be directly calculated with Eq. (10):

$$x_{b\_linear} = \frac{1}{2\phi} \cdot \frac{\Delta V}{t_r} \cdot \frac{L}{d} \cdot \tau_{pulse} \Delta z \tag{15}$$

Here, we see that for the case of a linear voltage ramp, the blur is not related to entrance time in the blanker, as may be expected. In other words, the amount of focal blur does not depend on whether the blanking aperture is placed on- or off-axis. However, a misalignment of the blanking aperture with respect to the axis will lead to a net displacement of the (blurred) focus with respect to the position of a non-deflected, continuous beam, as indicated in Fig. 3(b).

Furthermore, we see that besides electron beam parameters (energy and pulse duration), characteristics of the voltage pulse, and aspect ratio of the blanker, the blur depends linearly on the position of the focal plane with respect to the middle plane of the blanker. Misalignment of the focus in the blanker thus directly relates to focus blur on the sample.

Finally, we note that the blur is inversely proportional to the electron energy, under the condition that the same pulse duration is used. In general, changing the electron energy while keeping the blanker and voltage characteristics constant, will change the pulse duration proportionally, see Eq. (11). In fact, inserting Eq. (11) into Eq. (15) gives us a simple expression for the blur induced by a linear voltage ramp:

$$x_{b\_linear} = \frac{(d_{beam} + d_{aperature})}{H} \Delta z \tag{16}$$

Note that changing the electron energy will, in general, require a realignment of the conjugate focus in the blanker plates and thus Δz may change. As the change in beam diameter can typically be ignored, this is then the only way in which the blur is affected by the change in energy and, correspondingly, pulse duration. In the case where a non-linear voltage pulse is used for deflection, this simple picture may not hold anymore and one has to resort to evaluating Eq. (14) with the general expression in Eq. (9).

3. Results and discussion

Next, we illustrate the implications of the above derived equations using the parameters for a commercial beam blanker (FEI, now Thermo Fisher) that has been used in recent works [1,2,20,21]. In references [1,20,21], a FEI Quanta FEG 200 SEM was used with $L = 6.5$ mm, $d = 0.25$ mm, $H = 200$ mm, and a blanking aperture with diameter $d_{aperture} = 70$ μm. We consider the rising edge of the voltage inputs increasing from -5 V to 5 V as indicated in Fig. 1(a). As the electron pulse was obtained during the linear part of the voltage ramp, we can safely ignore the non-linear parts of $V(t)$. The maximum rise time reported by Moerland et al. [1] was about $t_r = 2.6$ ns, which would result in a pulse duration of 72 ps using Eq. (11) with an acceleration of 4 kV. The measured pulse duration reported in [1] was 90 ps for 4 kV, in good correspondence with the theoretical calculation considering the time jitter in the detection. Below we calculate SD and blur for a 5 kV acceleration voltage and blanker dimensions from the mentioned experimental papers.

3.1. Spot displacement

Inserting the above parameters into Eq. (10) we get:

$$x_{sd\_FEI} = 8.4 \cdot 10^{-7} + (1.22 \cdot 10^{-2} - 1 \cdot 10^7 t_{en}) \Delta z \tag{17}$$

The results of this Eq. (17) are shown in Fig. 4. As can be seen from this figure, the spot displacement is smallest when the focal plane is well aligned around the center of the beam blanker compared to misalignment towards entrance or exit of the blanker. With Eq. (17), we can also evaluate under which conditions the spot displacement is equal to zero:

$$z_{0\_linear} = \frac{1}{-1.43\cdot10^4 + 1.17\cdot10^{13}t_{en}} \tag{18}$$

which is shown in Fig. 4 with the red curves. We can further see that when the focus in the beam blanker is precisely aligned to the center plane, i.e. $\Delta z = 0$, the variable t_{en} falls out of the equation and the spot displacement has a constant value of $x_{sd\_linear} = 8.4\cdot10^{-7}$ m. This is indicated in Fig. 4 with a red dashed line. In this perfect situation, the blur induced in the focus by blanking will be zero.

The spot displacement in the blanker translates to a spot displacement on the sample plane according to:

$$x_{sdi} = M\cdot x_{sd} \tag{19}$$

where M is the demagnification from blanker to sample plane. In a typical experimental setup, $1/M = 20\sim30$. As can be seen in Fig. 4(b), the spot displacement is about 1 μm when the beam is focused roughly 100 μm from the middle plane of the blanker and the blanker aperture is aligned on-axis. In this case, the spot displacement in the sample plane is about 30~50 nm. If we estimate the diameter of the electron probe with the following equation [22]:

$$I_p = 2.47\frac{d_p^{3/8}B_r\phi}{C_s^{2/3}} \tag{20}$$

where we assume the spherical aberration coefficient to have a typical value of $C_s = 15$ mm, the reduced brightness of Schottky source $B_r = 2 \times 10^8$ A/(m²srV), an acceleration voltage of $\Phi = 5$ kV, and probe current $I_p = 10$ nA, we get $d_p = 8$ nm. Thus, the spot displacement on the sample when switching from continuous to pulsed beam operation can be several times the probe size.

If we assume that the electron beam is focused precisely in the middle plane of the blanker, i.e. $\Delta z = 0$, the spot displacement is simply related to the electron energy and distance between the blanker plates: $x_{sd0} = 7.4 \times 10^{-5}/(\phi^{3/2}\cdot d)$, which is shown in Fig. 5. It can be seen that there is hardly any relevant change of the spot displacement when electron energy is higher than 15 keV. For the smallest plate separation of d = 0.25 mm also used above, the full picture of spot displacement as a function of electron entrance time and focal misalignment is shown in Fig. 5(b-d) for energies of 10, 20, and 30 keV respectively. From the figure, it is obvious that the magnitude of spot displacement for increasing electron energy decreases and is also less impacted by misalignment or entry time with respect to the start of the voltage pulse. Higher energy electrons pass through the blanker faster and are therefore exposed to the deflection field for less time. The resulting smaller lateral velocity compared to low energy electrons makes for less deflection and thereby less spot displacement, as is also reflected in Eq. (10). However one should realize that changing electron energy (or plate separation), also increases the pulse duration, cf. Eq. (11). Thus, in order to evaluate the blur a wider range of electron entry times has to be evaluated. In fact, we have seen in Eq. (16) that the induced blur remains constant for varying electron energy, under the assumption of similar Δz.

3.2. Blur

Now, we turn to the evaluation of the blur induced in the focus, again for the case of $\Phi = 5$ keV and all other experimental parameters from reference [1], listed in the beginning of paragraph 3. We can directly evaluate the blur using Eq. (16) by using the diameter of the beam at the aperture plane, $d_{beam} = 2 \times \alpha \times H = 109\,\mu m$, where $\alpha = 0.27$ mrad at the center of beam blanker can be calculated with Eq. (21):

$$\alpha = \sqrt{\frac{4I_p}{B_r\pi^2\phi}}\cdot\frac{1}{d_g} \tag{21}$$

where d_g is the diameter of the electron beam at the center of beam blanker, $d_g = d_p/M = 240$ nm, assuming a probe diameter of ~8 nm

and a demagnification of M = 1/30.

Inserting into Eq. (16), we obtain a simple linear expression for the blur as a function of focal plane misalignment:

$$x_b = 9\cdot10^{-4}\Delta z \tag{22}$$

This relation is shown in Fig. 6. As can be seen, the blur in between the blanker plates can be in the order of several hundreds of nanometers when the focal misalignment is a few hundred micrometers. After demagnification by the objective lens, this can still mean a few tens of nanometers focus blur on the sample, significantly compromising resolution. Perfect alignment of the electron beam focus in the middle of the blanker leads to zero blur, which corresponds to constant spot displacement indicated in Fig. 4. Thus, careful alignment of the focus in the blanker plates needs to be done by evaluating image resolution as a function of the conjugate focus position in the blanker.

All our calculations here have been carried out for a linear increase in voltage, but other situations can be evaluated using the general spot displacement result in Eq. (14). Assuming a similar absolute voltage pulse and comparable rise time as above confirms the magnitude of spot displacement does not change significantly when using a sinusoidal or exponential pulse (see Supplemental Information). Conditions for constant spot displacement and thus zero blur can then be identified. However, for a non-linear pulse, the position of the blanking aperture with respect to the electron axis becomes more important. Aperture misalignment in case of a non-linear pulse will lead to different entry time for forward and backward deflected pulses (i.e. for the rising and falling edge of the voltage input) and thus to two displaced focus positions on the sample. Also, if the pulse is not symmetric around the zero-crossing, one must realize that the blur and spot displacement will be inverted for every other pulse in the sequence. This could potentially be solved by leading the electron beam around the aperture, or using an additional beam blanker for every other pulse.

Finally we note that our equations and results allow evaluation and optimization of the intrinsic limitations imposed by blanking. As mentioned in the introduction, a column design that is not optimized for having a conjugate focus at the position of the blanker and/or a small blanking aperture may add aberrations. Also, the experiments from which we extracted data to base our calculations on, were conducted with a few tens of pA, leading to < 0.1 electrons/pulse. Aiming for > 1 electron per pulse may lead to an additional loss of spatial resolution and also temporal pulse broadening due to Coulomb interactions in the pulse. However, in this case a blanker may still be a preferred solution compared to using a photo-emission gun in view of the shorter distance the pulse has to travel to reach the sample.

4. Conclusions

We have derived analytical expressions for the spot displacement induced by an electron beam blanker that consists of a single pair of electrostatic deflector plates. The general expression for spot displacement is given in Eq. (9) while Eq. (10) gives the result for the specific case that the blanker is driven by a linear voltage ramp. The spot displacement of the focus during blanking leads to a blur in the focus, which we showed can also be analysed using these equations. For a linear voltage ramp, this blur is zero when the conjugate focus is precisely aligned in the mid-plane of the blanker, and it increases linearly with misalignment. We have illustrated our results with a full calculation based on experimental variables from previously reported experiments where 90 ps pulses where obtained using a commercial beam blanker. In this specific case, with low electron energy (5 keV), we found a spot displacement of 30 nm under the condition of zero blur, i.e. perfect conjugate alignment, growing to ~50 nm with still only 3–4 nm blur when the conjugate focus in the blanker is 100 μm off from the mid-plane. Thus, the intrinsic loss in resolution imposed by using the blanker can be less than or equal to the magnitude of the probe (~5 nm). Our results allow to analyze this for any blanker design and
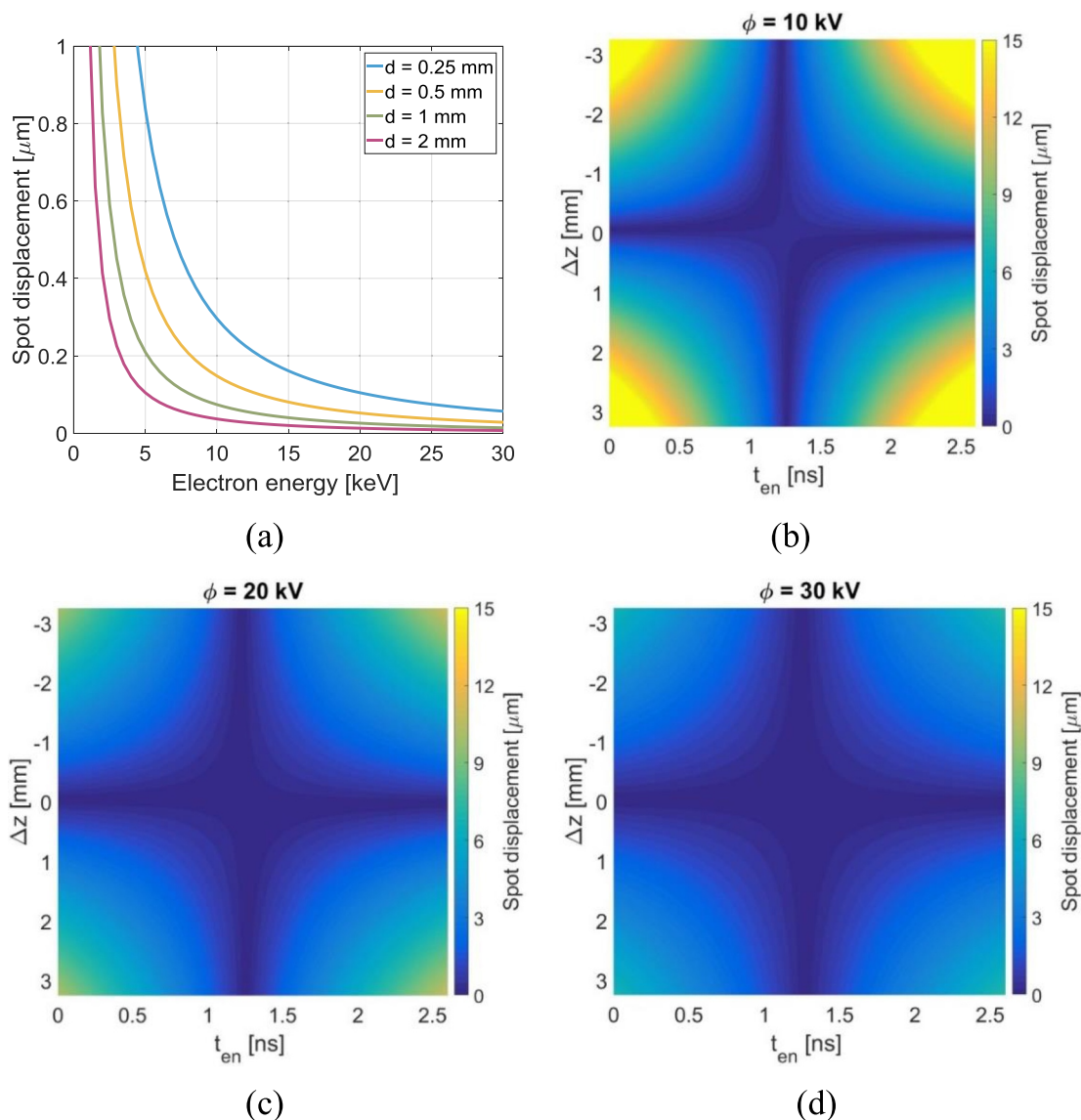
Fig. 5. (a) Variation of spot displacement with electron energy and deflector plate separation under condition of constant spot displacement (i.e. $\Delta z = 0$) and a linear voltage pulse. (b-d) Variation of the spot displacement with focal misalignment for the smallest plate separation of d = 0.25 mm. All other parameters as in Fig. 4 and listed at the beginning of paragraph 3. (This figure is available in color in the web version of this article).
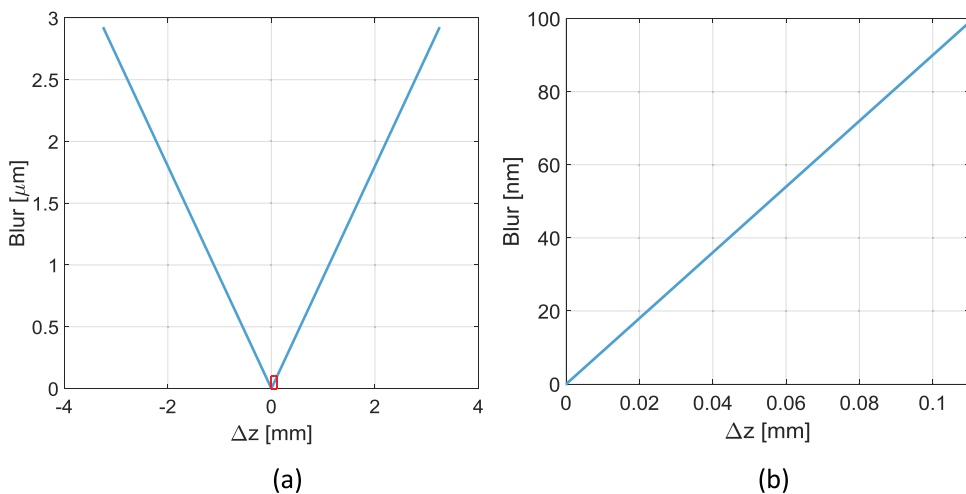
Fig. 6. (a) Blur induced at the blanker plane by a linear voltage input as a function of misalignment of the focal plane position with respect to the middle plane of the blanker. (b) Zoom-in of the red boxed region in (a). The blur is demagnified on the sample plane by the objective lens. The scale in (b) thus roughly corresponds to the regime in which the induced blur is of the same magnitude as the width of a high-resolution (~5 nm) probe beam. (For interpretation of the references to color in this figure legend, the reader is referred to the web version of this article.)

combination of experimental parameters and thus provide valuable guidelines for obtaining tens of picoseconds pulses in high resolution scanning electron microscopy.

Supplemental Information

In the Supplementary Information, we give the calculations of spot displacement and blur for three different shapes of the time dependence of the deflection voltage.

CRediT authorship contribution statement

Lixin Zhang: Methodology, Investigation, Formal analysis, Data curation, Supervision, Writing - original draft. **Mathijs W.H. Garming:** Writing - review & editing. **Jacob P. Hoogenboom:** Supervision, Writing - original draft, Writing - review & editing. **Pieter Kruit:** Supervision, Writing - review & editing.

Declaration of Competing Interest

The authors declare no competing interests.

Acknowledgments

Supplementary materials

Supplementary material associated with this article can be found, in the online version, at doi:10.1016/j.ultramic.2019.112925.

Reference

[1] R.J. Moerland, I.G.C. Weppelman, M.W.H. Garming, P. Kruit, J.P. Hoogenboom, Time-resolved cathodoluminescence microscopy with sub-nanosecond beam blanking for direct evaluation of the local density of states, Opt. Express 24 (2016) 24760.

[2] S. Meuret, M. Sola Garcia, T. Coenen, E. Kieft, H. Zeijlemaker, M. Latzel, S. Christiansen, S.Y. Woo, Y.H. Ra, Z. Mi, A. Polman, Complementary cathodoluminescence lifetime imaging configurations in a scanning electron microscope, Ultramicroscopy 197 (2019) 28–38.

[3] T.K. Fowler, W.M. Good, A theory on obtaining short bursts of ions from a beam of ions, Nucl. Instrum. Methods 7 (1960) 245–252.

[4] V. Auzelyte, M. Elfman, P. Kristiansson, K. Malmqvist, L. Wallman, C. Nilsson, J. Pallon, A. Shariff, M. Wegdén, The beam blanking system for microlithography at lund nuclear microprobe, Nucl. Instrum. Methods Phys. Res. Sect. B 219 (2004) 485–489.

[5] G.S. Plows, W.C. Nixon, Stroboscopic scanning electron microscopy, J. Sci. Instrum. 2 (1968) 595–600.

[6] K. Ura, H. Fujioka, T. Hosokawa, Picosecond pulse stroboscopic scanning electron microscope, J. Electron Microsc. 27 (1978) 256-256.

[7] J.T.L. Thong, B.C. Breton, W.C. Nixon, High repetition rate electron beam chopping system for electron beam testing at microwave frequencies, J. Vac. Sci. Technol. 8 (1990) 2048 B.

[8] D. Winkler, R. Schmitt, M. Brunner, B. Lischke, Flexible picosecond probing of integrated circuits with chopped electron beams, IBM J. Res. Dev. 34 (1990) 189–203.

[9] H. Sadorf, H.A. Kratz, Plug-in fast electron beam chopping system, Rev. Sci. Instrum. 56 (1985) 567–571.

[10] M. Gesley, An electron optical theory of beam blanking, Rev. Sci. Instrum. 64 (1993) 3169–3190.

[11] I.G.C. Weppelman, R.J. Moerland, J.P. Hoogenboom, P. Kruit, Concept and design of a beam blanker with integrated photoconductive switch for ultrafast electron microscopy, Ultramicroscopy 184 (2018) 8–17.

[12] I.G.C. Weppelman, R.J. Moerland, L. Zhang, E. Kieft, P. Kruit, J.P. Hoogenboom, Pulse length, energy spread, and temporal evolution of electron pulses generated with an ultrafast beam blanker, Struct. Dyn. 6 (2019) 024102.

[13] A. Lassise, P.H. Mutsaers, O.J. Luiten, Compact, low power radio frequency cavity for femtosecond electron microscopy, Rev. Sci. Instrum. 83 (2012) 043705.

[14] W. Verhoeven, J.F.M. van Rens, E.R. Kieft, P.H.A. Mutsaers, O.J. Luiten, High quality ultrafast transmission electron microscopy using resonant microwave cavities, Ultramicroscopy 188 (2018) 85–89.

[15] J.F.M. Van Rens, W. Verhoeven, J.G. Franssen, A.C. Lassise, X.F.D. Stragier, E.R. Kieft, P.H.A. Mutsaers, O.J. Luiten, Theory and particle tracking simulations of a resonant radiofrequency deflection cavity in TM_{110} mode for ultrafast electron microscopy, Ultramicroscopy 184 (2017) 77.

[16] L. Zhang, J.P. Hoogenboom, B. Cook, P. Kruit, Photoemission sources and beam blankers for ultrafast electron microscopy, Struct. Dyn. 6 (2019) 051501.

[17] H. Paik, E.J. Kirkland, B.M. Siegel, Analytical calculation of electrostatic beam blanker performance, J. Phys. E 20 (1987) 61–66.

[18] E. Mulder, P. Kruit, Spot movement due to signal transients in multiple deflector blankers in electron beam lithography machines, Microelectron. Eng. 41 (1998) 159–162.

[19] J. Ruan, Electron Beam Lithography Throughput and Resolution Enhancement with Innovative Blanker Design, Ph.D. thesis State University of New York, 2010.

[20] M.W.H. Garming, I.G.C.W. Weppelman, P. De Boer, F.P. Martínez, R. Schirhagl, J.P. Hoogenboom, R.J. Moerland, Nanoparticle discrimination based on wavelength and lifetime-multiplexed cathodoluminescence microscopy, Nanoscale 9 (2017) 12727–12734.

[21] R.J. Moerland, I.G.C. Weppelman, M. Scotuzzi, J.P. Hoogenboom, Nanoscale imaging of light-matter coupling inside metal-coated cavities with a pulsed electron beam, Nano Lett. 18 (2018) 6107–6112.

[22] P. Kruit, M. Bezuijen, J.E. Barth, Source brightness and useful beam current of carbon nanotubes and other very small emitters, J. Appl. Phys. 99 (2006) 024315.